

Evaluation of Biofield Treatment on Atomic and Thermal Properties of Ethanol

Mahendra Kumar Trivedi¹, Alice Branton¹, Dahryn Trivedi¹, Gopal Nayak¹, Omprakash Latiyal² and Snehasis Jana^{2*}

¹Trivedi Global Inc., 10624 S Eastern Avenue Suite A-969, Henderson, NV 89052, USA

²Trivedi Science Research Laboratory Pvt. Ltd., Hall-A, Chinar Mega Mall, Chinar Fortune City, Hoshangabad Rd., Bhopal, Madhya Pradesh, India

Abstract

Ethanol is a polar organic solvent, and frequently used as a fuel in automobile industries, principally as an additive with gasoline due to its higher octane rating. It is generally produced from biomass such as corn, sugar and some other agriculture products. In the present study, impact of biofield treatment on ethanol was evaluated with respect to its atomic and thermal properties. The ethanol sample was divided into two parts i.e., control and treatment. Control part was remained untreated. Treatment part was subjected to Mr. Trivedi's biofield treatment. Control and treated samples were characterized using Gas chromatography-mass Spectrometry (GC-MS), Differential scanning calorimetry (DSC), and High performance liquid chromatography (HPLC). GC-MS data revealed that isotopic abundance of ¹³C i.e., δ¹³C of treated ethanol was significantly changed from -199‰ upto 155‰ as compared to control. The DSC data exhibited that the latent heat of vaporization of treated ethanol was increased by 94.24% as compared to control, while no significant change was found in boiling point. Besides, HPLC data showed that retention time was 2.65 minutes in control, was increased to 2.76 minutes in treated ethanol sample. Thus, overall data suggest that biofield treatment has altered the atomic and thermal properties of ethanol.

Keywords: Biofield treatment; Ethanol; Gas Chromatography-Mass Spectrometry; Differential scanning calorimetry; High performance liquid chromatography

Introduction

Ethanol or ethyl alcohol (C₂H₅OH) is a clear, volatile, colourless, and polar organic solvent. It is a source of energy being utilized with petrol/gasoline for vehicle fuel. Recently, the conventional fuel prices are increasing continuously, and further due to their limited natural resource; there is a huge demand to utilize the renewable biofuels produced from agriculture products. It is expected that, around 20% of petroleum will be replaced by another fuel in next 10 years [1]. Hence, the ethanol being a renewable source of energy, will play an important role in future. The ethanol fuel has very high octane rating than petrol, diesel, and gasoline. The high octane rating indicates the high fuel efficiency by mean of less premature combustion and prevents spark ignition. Ethanol contains 35% w/w oxygen, which assists gasoline to burn completely in ethanol-gasoline blend fuel. This complete combustion of ethanol-gasoline fuel reduces the gummy deposits in engines. Despite of all these positive benefits, the ethanol has less energy content than gasoline and petrol. From several decades ethanol has been produced as a by-product from sugar industries and is being used in beverage industry. Recently, ethanol has been synthesized from corn starch, wheat and other plant products. Zyakum et al. reported that carbon isotopic ratio ¹³C/¹²C of ethanol produced by fragmentation technique depends upon the substrate used, for instance, the ethanol produced using wheat as substrate was found lesser than cereals [2,3]. Besides, isotopic fractionation in a product can be changed through chemical reactions or a physicochemical process. The change in isotopic ratio ¹³C/¹²C, affects the compound in two ways i.e., thermodynamic and kinetic isotopic. In kinetic isotope effect (KIE), different isotopes of same element are present in any compound, which have different bond length and bond strength. Furthermore, in a chemical reaction breaking of bonds plays a significant role, which ultimately determines the rate of a reaction. The thermodynamic isotopic effect concerns with the physicochemical properties such as heat of vaporization, boiling point, and vapor pressure. After considering of ethanol properties and fuel applications, authors wanted to investigate an approach that could be beneficial to modify the atomic and thermal properties of ethanol.

According to William Tiller, a physicist, proposed the existence of a new force related to human body, in addition to four well known fundamental forces of physics: gravitational force, strong force, weak force, and electromagnetic force [4]. A biophysicist Fritz-Albert Popp proposed that human physiology shows a high degree of order and stability due to their coherent dynamic states [5-8]. This emits the electromagnetic (EM) waves in form of bio-photons, which surrounds the human body and it is commonly known as biofield. Furthermore, a human has ability to harness the energy from environment/universe and it can transmit into any object (living or non-living) on the Globe. The object always receives the energy and responded into useful way, which known as biofield energy. This process is called biofield treatment. Mr. Trivedi's biofield treatment ('The Trivedi Effect') is well known to transform the characteristics in various fields such as material science [9-11], agriculture [12-14], microbiology [15-17], and biotechnology [18,19]. Biofield treatment has shown significant alteration in metals [20-22] and ceramics [23,24] with respect to their atomic and structural properties. Based on the excellent result obtained by biofield treatment in material science, the present study was undertaken to evaluate the impact of biofield treatment on atomic and thermal properties of ethanol.

Experimental

The ethanol sample used in this experiment was procured from Sigma Aldrich, China. The ethanol sample was distributed into two

***Corresponding author:** Snehasis Jana, Trivedi Science Research Laboratory Pvt. Ltd., Hall-A, Chinar Mega Mall, Chinar Fortune City, Hoshangabad Rd., Bhopal- 462026, Madhya Pradesh, India, Tel: 917556660006; E-mail: publication@trivedisrl.com

Received: August 03, 2015; **Accepted:** August 12, 2015; **Published:** August 20, 2015

Citation: Trivedi MK, Branton A, Trivedi D, Nayak G, Latiyal O, et al. (2015) Evaluation of Biofield Treatment on Atomic and Thermal Properties of Ethanol. Organic Chem Curr Res 4:145. doi:[10.4172/2161-0401.1000145](http://dx.doi.org/10.4172/2161-0401.1000145)

Copyright: © 2015 Trivedi MK, et al. This is an open-access article distributed under the terms of the Creative Commons Attribution License, which permits unrestricted use, distribution, and reproduction in any medium, provided the original author and source are credited.

equal parts, where one part was referred as control sample and another part was subjected to Mr. Trivedi's biofield treatment, which was considered as treated sample. The control and treated samples were characterized using Gas chromatography-mass spectrometry (GC-MS), Differential scanning calorimetry (DSC), and High performance liquid chromatography (HPLC) techniques.

Gas Chromatography-Mass Spectrometry

The gas chromatography-mass spectroscopy (GC-MS) analysis was performed on Perkin Elmer/auto system XL with Turbo mass, USA, having detection limit up to 1 picogram. For GC-MS analysis the treated sample was further divided into three parts as T1, T2 and T3. The GC-MS data was obtained in the form of % abundance vs. mass to charge ratio (m/z), which is known as mass spectrum. The isotopic abundance of ^{13}C was expressed by its deviation in treated ethanol sample as compared to control. Isotopic abundance of ^{13}C i.e., $\delta^{13}\text{C}$ was computed on thousand scale using equation as following:

$$\delta^{13}\text{C} (\text{‰}) = \frac{R_{\text{Treated}} - R_{\text{Control}}}{R_{\text{Control}}} \times 1000 \quad (1)$$

Where, R_{Treated} and R_{Control} are the ratio of intensity at $m/z=47$ to $m/z=46$ in mass spectra of treated and control samples respectively.

Differential scanning calorimetry

For thermal analysis, Differential Scanning Calorimeter (DSC) of Perkin Elmer/Pyris-1, USA, with a heating rate of $10^\circ\text{C}/\text{min}$ and nitrogen flow of $5 \text{ mL}/\text{min}$ was used. The boiling point and latent heat of vaporization of control and treated ethanol was recorded from their respective DSC curves. The percent change in boiling point and latent heat of vaporization was computed using following equations: Percent change in melting point was calculated using following equations:

$$\% \text{ change in boiling point} = \frac{[T_{\text{Treated}} - T_{\text{Control}}]}{T_{\text{Control}}} \times 100$$

Where, T_{Control} and T_{Treated} are the boiling point of control and treated samples, respectively.

Percent change in latent heat of vaporization was calculated using following equations:

$$\% \text{ change in Latent heat of vaporization} = \frac{[\Delta H_{\text{Treated}} - \Delta H_{\text{Control}}]}{\Delta H_{\text{Control}}} \times 100$$

Where, $\Delta H_{\text{Control}}$ and $\Delta H_{\text{Treated}}$ are the latent heat of vaporization of control and treated samples, respectively.

High performance liquid chromatography

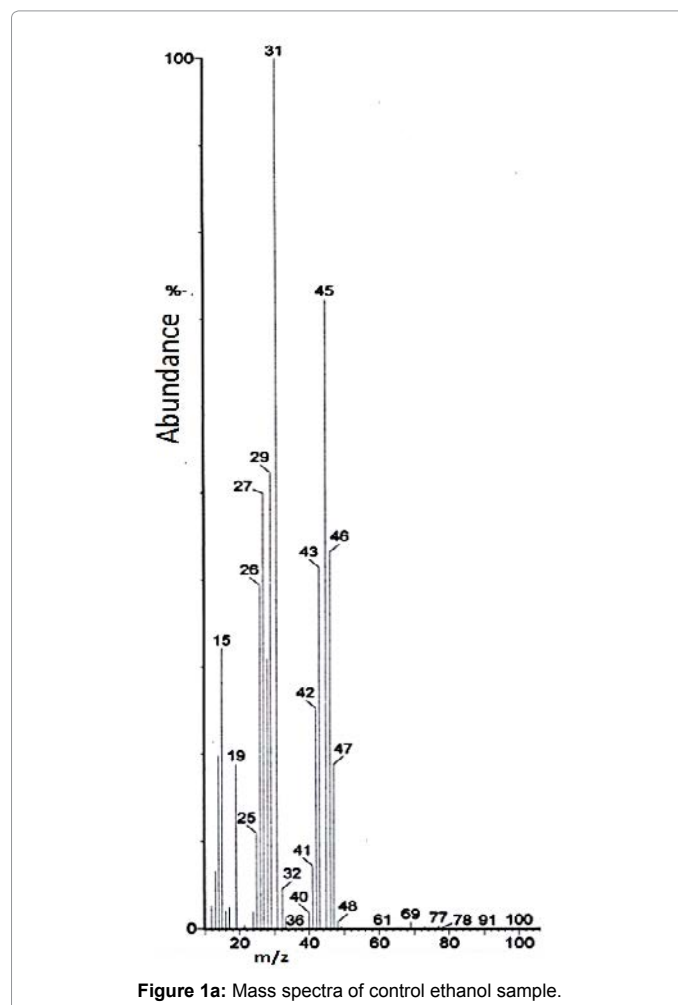
The HPLC analysis was performed on a Knauer High Performance Liquid Chromatograph (Berlin, Germany), which consists of a solvent delivery system Smartline Pump 1000 equipped with a UV 2600 detector. Chromatographic separation was achieved on a C_{18} column (Eurospheer 100) with a dimension of $250 \times 4 \text{ mm}$ and $5 \mu\text{m}$ particle size. The mobile phase used was methanol with a flow rate of $1 \text{ mL}/\text{min}$.

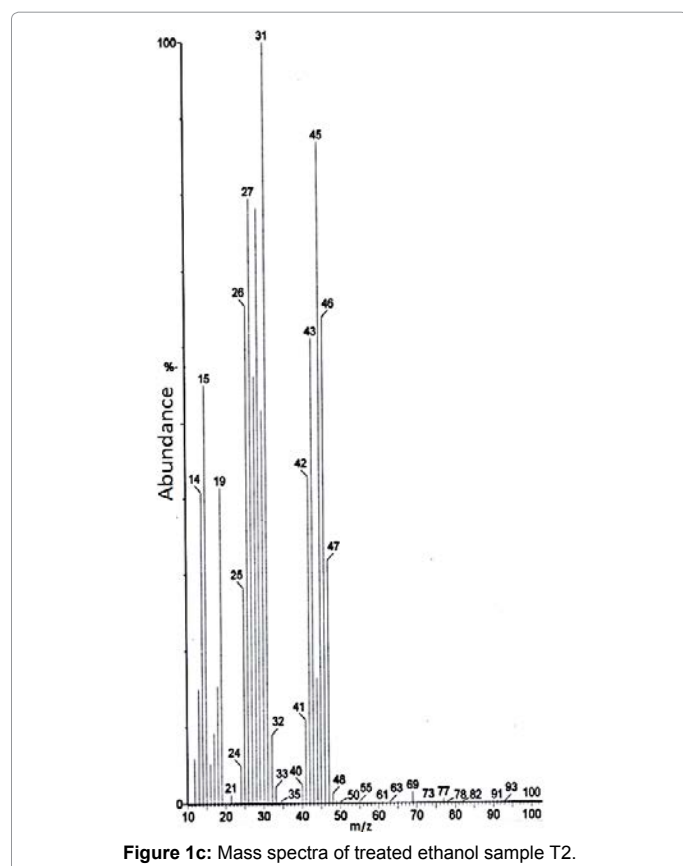
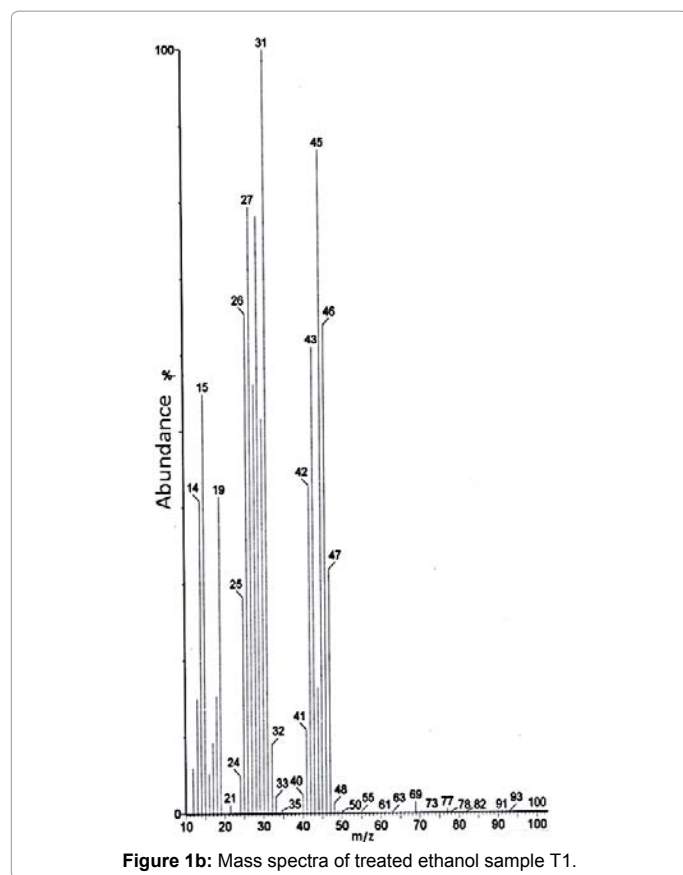
Results and Discussion

Gas Chromatography-Mass Spectrometry

The mass spectrum of control and treated samples (T1, T2 and T3) of ethanol are shown in Figure 1a-1c. In mass spectra of control and treated ethanol samples, different intensities were observed. Mass spectra showed that base peak at $m/z=45$ in control sample (Figure 1a),

whereas in treated samples the base peaks were found at $m/z=31$ in T1, T2, and T3 (Figure 1b-1c). Furthermore, the intense peaks with different mass to charge ratio (m/z), of possible molecular ions are illustrated in Table 1. It indicates that peak at $m/z=31$ and $m/z=45$ were due to $^{12}\text{CH}_2\text{OH}^+$ and $^{12}\text{C}_2\text{H}_4\text{OH}^+$, respectively in control and treated samples. Peaks at $m/z=46$ correspond to ethanol ion with carbon-12 ($^{12}\text{CH}_3\text{-}^{12}\text{CH}_2\text{O}^+\text{H}^+$), whereas the peak at $m/z=47$ corresponds to ethanol ion with carbon-13 i.e., $^{13}\text{CH}_3\text{-}^{12}\text{CH}_2\text{OH}^+$ or $^{12}\text{CH}_3\text{-}^{13}\text{CH}_2\text{OH}^+$. Computed result of isotopic ratio, $^{13}\text{C}/^{12}\text{C}$ from GC-MS spectra are presented in Table 2. Further, the isotopic abundance $\delta^{13}\text{C}$ computed using equation (1) is illustrated in Figure 2. It showed that the $\delta^{13}\text{C}$ was significantly increased by 5‰ and 155‰ (per 1000) in sample T1 and T3, respectively, while it was reduced by 199‰ in T2 as compared to control. This suggests that the ^{12}C atoms of T1 and T3, probably transformed into ^{13}C by capturing one neutron thereby increased $\delta^{13}\text{C}$. Whereas in T2, the ^{13}C atoms probably transformed into ^{12}C by emitting one neutron and reduced $\delta^{13}\text{C}$. This inter-conversion of ^{13}C and ^{12}C can be possible if a nuclear level reaction including the neutron and proton occurred after biofield treatment. Thus, it is assumed that biofield treatment possibly induced the nuclear level reactions, which may lead to alter the isotopic ratio $^{13}\text{C}/^{12}\text{C}$ in treated ethanol. Besides, it is reported that when lighter isotope (^{12}C) is substituted with heavier (^{13}C) in any compound or *vice versa*, it doesn't affect the nuclear charge and electronic structure, since ^{12}C and ^{13}C atoms are differentiated by one neutron, which is a neutral particle [25]. Thus the vibrational



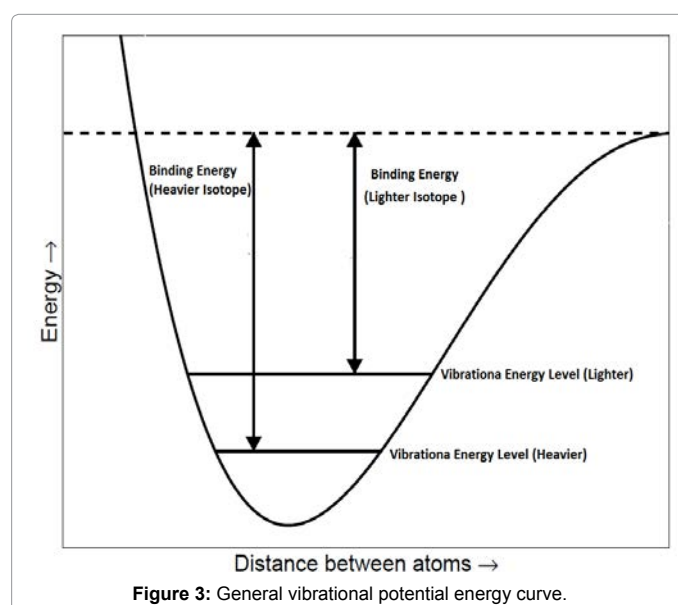
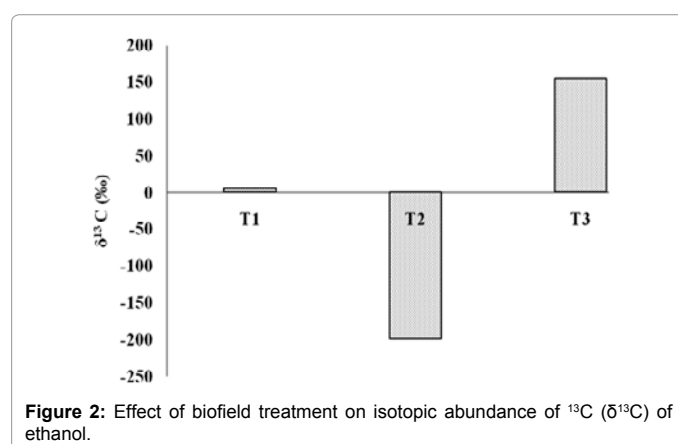


| Ratio <i>m/z</i> | Possible detected molecules |
|------------------|---|
| 29 | $^{12}\text{C}_2\text{H}_5^+$ |
| 31 | $^{12}\text{CH}_2\text{OH}^+$ |
| 45 | $^{12}\text{C}_2\text{H}_4\text{OH}^+$ |
| 46 | $^{12}\text{CH}_3\text{-}^{12}\text{CH}_2\text{-}^{16}\text{O}^1\text{H}^+$ |
| 47 | $^{13}\text{CH}_3\text{-}^{12}\text{CH}_2\text{OH}^+$ or $^{12}\text{CH}_3\text{-}^{13}\text{CH}_2\text{OH}^+$ |
| 48 | $^{13}\text{CH}_3\text{-}^{13}\text{CH}_2\text{OH}^+$ or $^{13}\text{CH}_3\text{-}^{12}\text{CH}_2\text{-}^{17}\text{OH}^+$ |

Table 1: Identification of peaks in MS spectra of ethanol.

| Parameters | Control | T1 | T2 | T3 |
|---|---------|--------|--------|--------|
| Peak Intensity at <i>m/z</i> = 46 | 60.47 | 43.16 | 62.16 | 63.78 |
| Peak Intensity at <i>m/z</i> = 47 | 26.13 | 18.75 | 21.51 | 31.85 |
| Ratio of peak intensity at <i>m/z</i> = 47 to <i>m/z</i> = 46 | 0.4321 | 0.4344 | 0.3460 | 0.4993 |

Table 2: GC-MS isotopic abundance analysis result of ethanol.



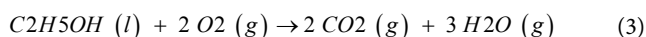
potential energy curve remains same (Figure 3). Furthermore, the vibration energy level of a bond in a molecule can be represented by following equation [26].

$$E = \frac{(n+1)h\left(\frac{k}{\mu}\right)^{\frac{1}{2}}}{2\pi} \quad (2)$$

Where, n is quantum number ($=0, 1, 2 \dots$), h is Plank's constant, k is bond constant and μ is the reduced mass $=M_A \times M_B / (M_A + M_B)$

Where M_A and M_B are the atomic mass of atoms A and B respectively, which forms the bond A-B.

According to the equation (2) vibration energy level is inversely proportional to reduced mass. Furthermore, it is well known that the lower is the vibration energy level, higher the stability of molecules. Typically, in ethanol, many type of bonds are present such as $^{12}\text{C}-^{12}\text{C}$, $^{13}\text{C}-^{12}\text{C}$, $^1\text{H}-^{12}\text{C}$, $^1\text{H}-^{13}\text{C}$, $^{12}\text{C}-^{16}\text{O}$, $^{13}\text{C}-^{16}\text{O}$, and $^{16}\text{O}-^1\text{H}$ and reduced mass of these bond are illustrated in Table 3. It showed that reduced mass was higher in case of heavier isotope as compared to lighter. This indicates that ethanol with heavier isotope have low vibration energy level and more stability as compared to lighter ones. Furthermore, the higher stability of ethanol with heavier isotopes may lead to increase the enthalpy of reaction for combustion with oxygen. (Equation 3) This enthalpy of reaction is also known as heat of combustion of ethanol fuel.



In case of treated ethanol, the amount of heavier isotopic ^{13}C atoms was significantly changed after biofield treatment. Thus, it is assumed that ethanol samples with higher isotopic abundance $\delta^{13}\text{C}$ (T1 and T3) might have higher stability and binding energy as compared to control [26]. In addition, the higher binding energy of treated ethanol may lead to increase the heat of combustion. On contrary, reverse might happen in treated T2. Thus, GC-MS data suggest that biofield treatment has significantly altered the isotopic abundance of ^{13}C in treated ethanol samples.

Differential scanning calorimetry (DSC)

DSC was used for thermal analysis of control and treated ethanol samples. DSC curve of control and treated ethanol (T1) are shown in Figure 4a and 4b, respectively. Analysis result of boiling point and latent heat of vaporization (ΔH) are presented in Table 4. Data showed that boiling temperature of ethanol was slightly reduced from 77.47°C (control) to 76.95°C after biofield treatment. Whereas, the latent heat of vaporization (ΔH) was increased from 253 J/g (control) to 499.2 J/g in treated ethanol sample. It indicated that the ΔH of treated ethanol was significantly increased by 94.24% as compared to control. The increase in ΔH after biofield treatment could be due to higher intermolecular interaction in ethanol molecules in treated sample as compared to control. Furthermore, the increase in intermolecular interaction may enhance the thermal stability of ethanol after biofield treatment.

High performance liquid chromatography (HPLC)

HPLC chromatogram of control and treated ethanol (T1) is shown in Figure 5a and 5b, respectively. The control ethanol showed a retention time (R_t) at 2.65 min, however after biofield treatment, it was shifted to 2.76 min. This increased (shift) of retention time can be attributed to reduced polarity of ethanol after treatment. Further, the decreased polarity after biofield treatment may be due to more interaction of treated ethanol with non-polar silica phase in C18 column that resulted into higher retention time. It is presumed that biofield treatment probably acting at atomic level, which reduced the electronegativity of oxygen atom present in ethanol and that might be responsible to decrease polarity. Due to this, hygroscopicity of treated ethanol might be reduced after biofield treatment. Thus, the reduced hygroscopic nature of treated ethanol might prevent the dilution of ethanol from moisture, which could maintain the purity of ethanol fuel with high energy content.

Conclusion

In summary, the biofield treatment has significantly changed the isotopic abundance of ^{13}C and latent heat of vaporization in ethanol. The GC-MS data showed that biofield treatment has significantly changed the isotopic abundance of ^{13}C i.e., $\delta^{13}\text{C}$ from -199‰ upto 155‰ in treated ethanol as compared to control. It could be due to nuclear level transformation of ^{13}C and ^{12}C , which probably induced through biofield treatment. Moreover, the higher $\delta^{13}\text{C}$ in treated ethanol may increase the stability of bonds, binding energy and heat of combustion. Besides, DSC data suggest that latent heat of vaporization of treated ethanol sample was increased by 94.24% as compared to

| Isotopes Bonds | Isotope type | Reduced mass ($M_A M_B / (M_A + M_B)$) |
|-------------------------------|--------------|--|
| $^{12}\text{C}-^{12}\text{C}$ | Lighter | 6.00 |
| $^{13}\text{C}-^{12}\text{C}$ | Heavier | 6.24 |
| $^1\text{H}-^{12}\text{C}$ | Lighter | 0.923 |
| $^1\text{H}-^{13}\text{C}$ | Heavier | 0.928 |
| $^{12}\text{C}-^{16}\text{O}$ | Lighter | 6.85 |
| $^{13}\text{C}-^{16}\text{O}$ | Heavier | 7.17 |
| $^{16}\text{O}-^1\text{H}$ | Lighter | 0.94 |
| $^{16}\text{O}-^2\text{H}$ | Heavier | 1.77 |

Table 3: Possible isotopic bonds in ethanol.

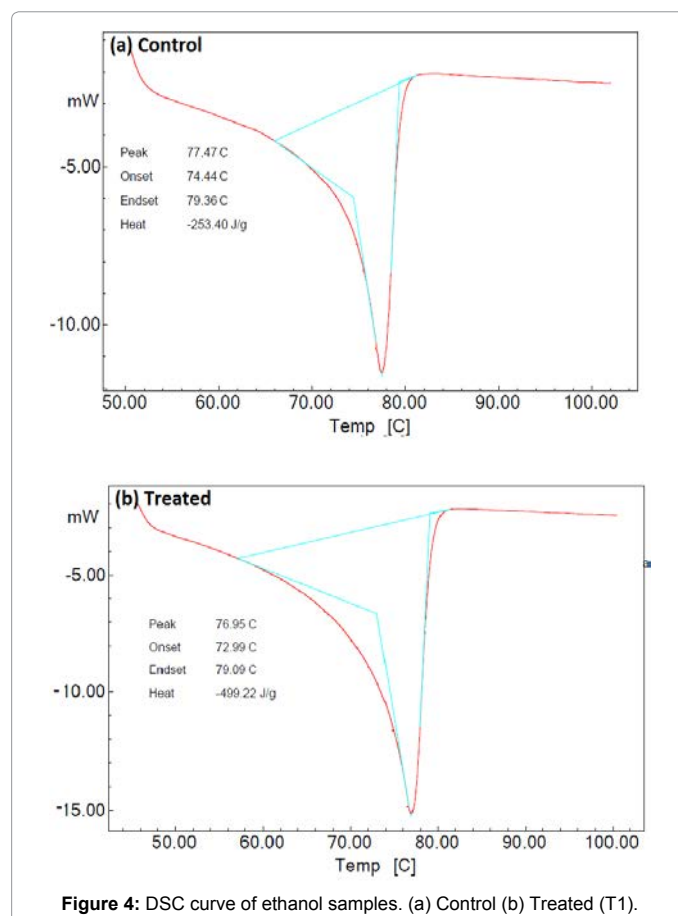


Figure 4: DSC curve of ethanol samples. (a) Control (b) Treated (T1).

| Parameters | Control | Treated (T1) | Percent Change |
|-----------------------------------|---------|--------------|----------------|
| Boiling point (°C) | 77.47 | 76.95 | -0.67 |
| Latent heat of vaporization (J/g) | 253.4 | 492.22 | 94.24 |

Table 4: DSC analysis data of control and treated ethanol.

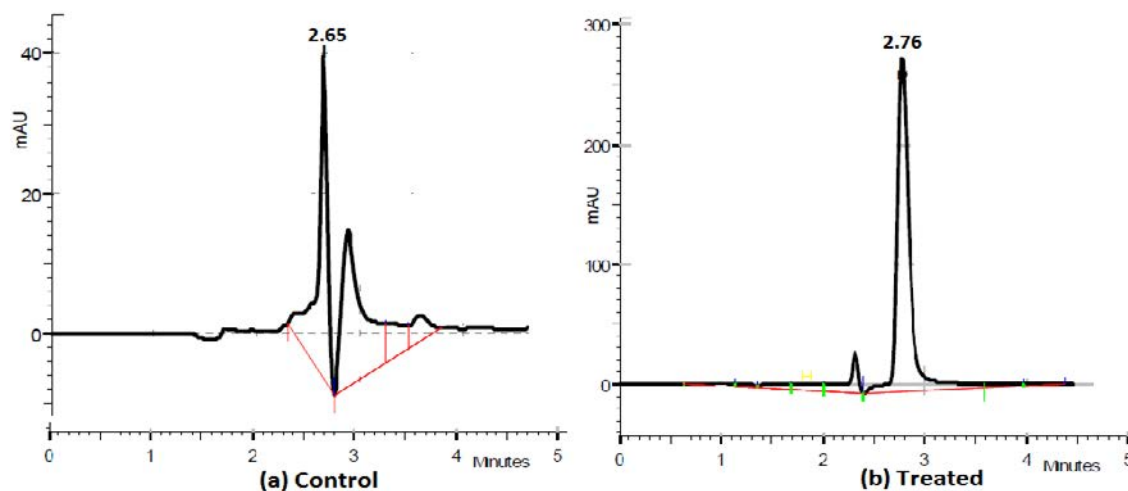


Figure 5: HPLC spectra of ethanol samples. (a) Control (b) Treated (T1).

control, which may be due to improved thermal stability of ethanol after biofield treatment. Nevertheless, the shift in retention time toward higher side in HPLC spectra of treated as compared to control revealed that the polarity of ethanol possibly reduced after biofield treatment, which may diminished the hygroscopic nature of ethanol. Therefore, the biofield treated ethanol with high energy content and lower hygroscopic nature could be utilized as a fuel in automobiles.

Acknowledgements

We thank to all the staff of concern Laboratories, who supported us in conducting experiments. Authors also would like to thank Trivedi Science, Trivedi master wellness and Trivedi testimonials for their support during the work.

References

1. Wen Z, Ignosh J, Arogo J (2009) Fuel ethanol. *Virginia Tech* 2009: 442-884.
2. Zyakun AM, Zakharchenko VN, Kudryavtseva AI, Peshenko VP, Mashkina LP et al. (2000) The use of $^{13}\text{C}/^{12}\text{C}$ isotope abundance ratio for characterization of the origin of ethyl alcohol. *Appl Biochem Microbiol* 36: 11-14.
3. Kirichenko EB, Zyakun AM, Bondar VA, Kirichenko AB, Bezruchko VV, et al. (1980) Ratio of stable carbon isotopes ($^{13}\text{C}/^{12}\text{C}$) in vegetative and generative organs of plants of the grass family. *Doklady, botanical sciences*. 250: 505-508.
4. Tiller WA (1997) *Science and human transformation: subtle energies, intentionality and consciousness* (1st edn). Pavior Publishing, Walnut Creek, California.
5. Popp FA, Chang JJ, Herzog A, Yan Z, Yan Y (2002) Evidence of non-classical (squeezed) light in biological systems. *Phys Lett* 293: 98-102.
6. Popp FA, Gu Q, Li KH (1994) Biophoton emission: Experimental background and theoretical approaches. *Mod Phys Lett B* 8: 21-22.
7. Popp FA (1992). *Recent advances in biophoton research and its applications*. World Scientific Publishing Co Pte Ltd.
8. Cohen S, Popp FA (2003) Biophoton emission of human body. See comment in PubMed Commons below *Indian J Exp Biol* 41: 440-445.
9. Trivedi MK, Tallapragada RM (2008) A transcendental to changing metal powder characteristics. *Met Powder Rep* 63: 22-28.
10. Trivedi MK, Tallapragada RM (2009) Effect of super consciousness external energy on atomic, crystalline and powder characteristics of carbon allotrope powders. *Mater Res Innov* 13: 473-480.
11. Dhabade VV, Tallapragada RM, Trivedi MK (2009) Effect of external energy on atomic, crystalline and powder characteristics of antimony and bismuth powders. *Bull Mater Sci* 32: 471-479.
12. Shinde V, Sances F, Patil S, Spence A (2012) Impact of biofield treatment on growth and yield of lettuce and tomato. *Aust J Basic Appl Sci* 6: 100-105.
13. Lenssen AW (2013) Biofield and fungicide seed treatment influences on soybean productivity, seed quality and weed community. *Agricultural Journal* 8: 138-143.
14. Sances F, Flora E, Patil S, Spence A, Shinde V, et al. (2013) Impact of biofield treatment on ginseng and organic blueberry yield. *Agrivita J Agric Sci* 35.
15. Trivedi MK, Patil S, Bhardwaj Y (2008) Impact of an external energy on *Staphylococcus epidermis* [ATCC-13518] in relation to antibiotic susceptibility and biochemical reactions - An experimental study. *J Accord Integr Med* 4: 230-235.
16. Trivedi MK, Patil S (2008) Impact of an external energy on *Yersinia enterocolitica* [ATCC -23715] in relation to antibiotic susceptibility and biochemical reactions: An experimental study. *Internet J Alternat Med* 6.
17. Trivedi MK, Patil S, Bhardwaj Y (2009) Impact of an external energy on *Enterococcus faecalis* [ATCC-51299] in relation to antibiotic susceptibility and biochemical reactions - An experimental study. *J Accord Integr Med* 5: 119-130.
18. Patil S, Nayak GB, Barve SS, Tembe RP, Khan RR, et al. (2012) Impact of biofield treatment on growth and anatomical characteristics of *Pogostemoncablin* (Benth.). *Biotechnology* 11: 154-162.
19. Altekar N, Nayak G (2015) Effect of biofield treatment on plant growth and adaptation. *J Environ Health Sci* 1: 1-9.
20. Trivedi MK, Patil S, Tallapragada RM (2012) Thought Intervention through bio field changing metal powder characteristics experiments on powder characteristics at a PM plant. *Future Control and Automation LNEE* 173: 247-252.
21. Trivedi MK, Patil S, Tallapragada RM (2015) Effect of biofield treatment on the physical and thermal characteristics of aluminium powders. *Ind Eng Manage* 4: 151.
22. Trivedi MK, Patil S, Tallapragada RM (2013) Effect of biofield treatment on the physical and thermal characteristics of silicon, tin and lead powders. *J Material Sci Eng* 2: 125.
23. Trivedi MK, Patil S, Tallapragada RM (2013) Effect of biofield treatment on the physical and thermal characteristics of vanadium pentoxide powder. *J Material Sci Eng* S11: 001.
24. Trivedi MK, Patil S, Tallapragada RM (2014) Atomic, crystalline and powder characteristics of treated zirconia and silica powders. *J Material Sci Eng* 3: 144.
25. Wilson EB, Decius JC, Cross PC (1995) *Molecular Vibrations*. New York: Dover.
26. Califano S (1976). *Vibrational States*. New York: Wiley.

Citation: Trivedi MK, Branton A, Trivedi D, Nayak G, Latiyal O, et al. (2015) Evaluation of Biofield Treatment on Atomic and Thermal Properties of Ethanol. *Organic Chem Curr Res* 4:145. doi:10.4172/2161-0401.1000145